

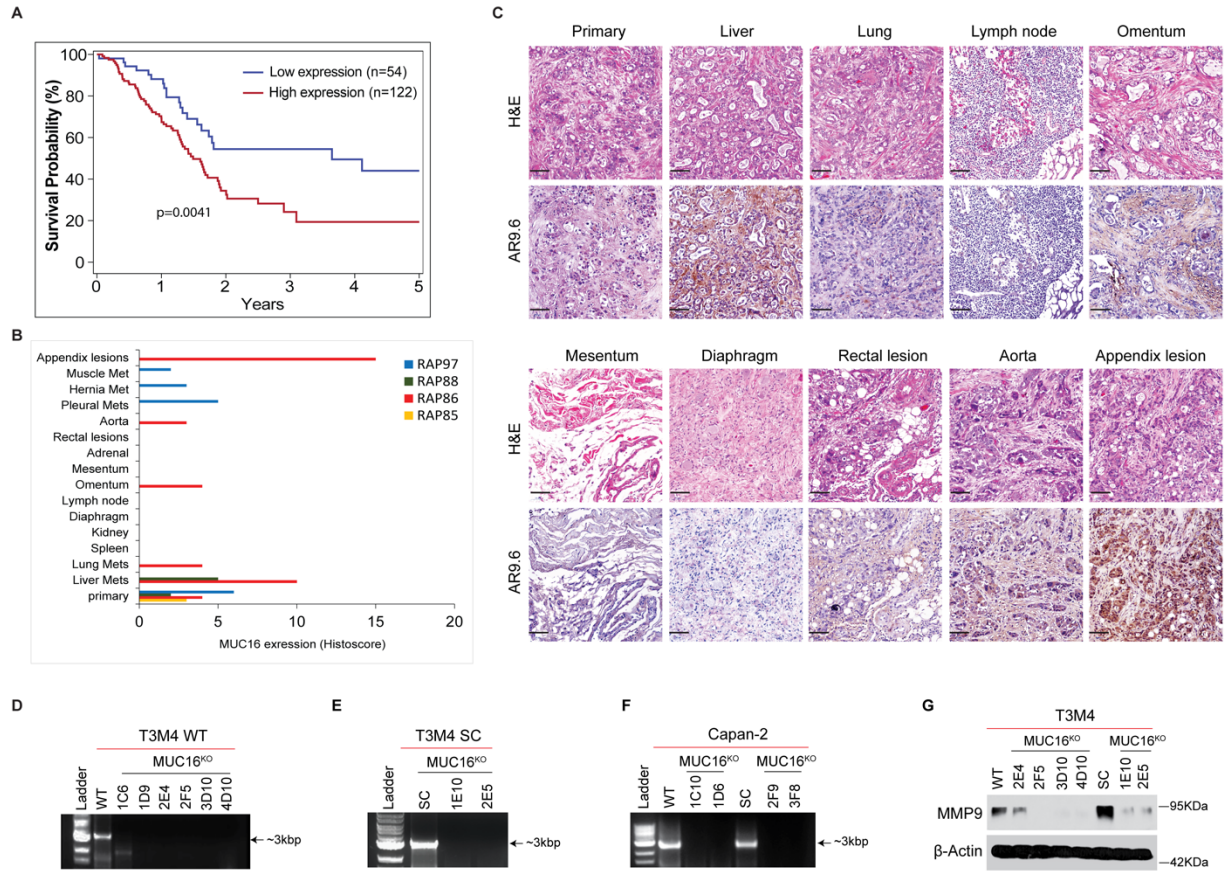
Supplemental Information

Isoforms of MUC16 activate oncogenic signaling through EGF receptors to enhance the progression of pancreatic cancer

Divya Thomas, Satish Sagar, Xiang Liu, Hye-Rim Lee, James A. Grunkemeyer, Paul M. Grandgenett, Thomas Caffrey, Kelly A. O'Connell, Benjamin Swanson, Lara Marcos-Silva, Catharina Steentoft, Hans H. Wandall, Hans Carlo Maurer, Xianlu Laura Peng, Jen Jen Yeh, Fang Qiu, Fang Yu, Ragupathy Madiyalakan, Kenneth P. Olive, Ulla Mandel, Henrik Clausen, Michael A. Hollingsworth, and Prakash Radhakrishnan

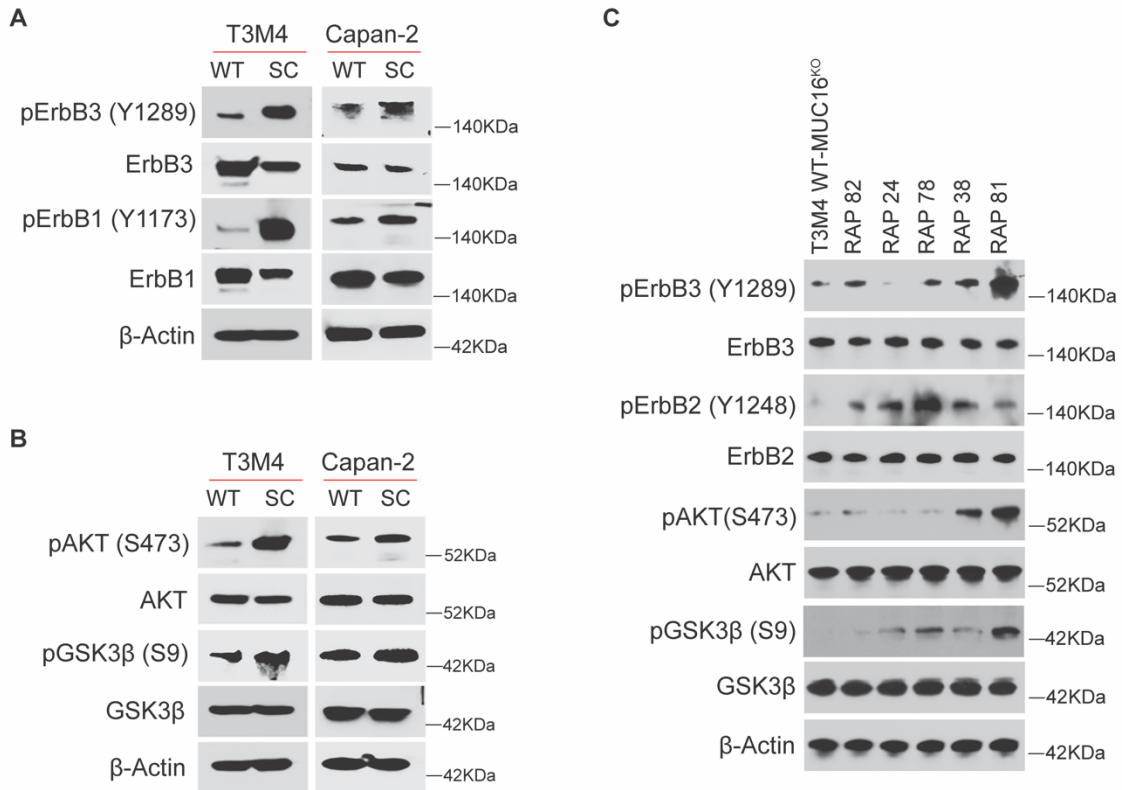
Supplemental Figures

Supplementary Figure 1



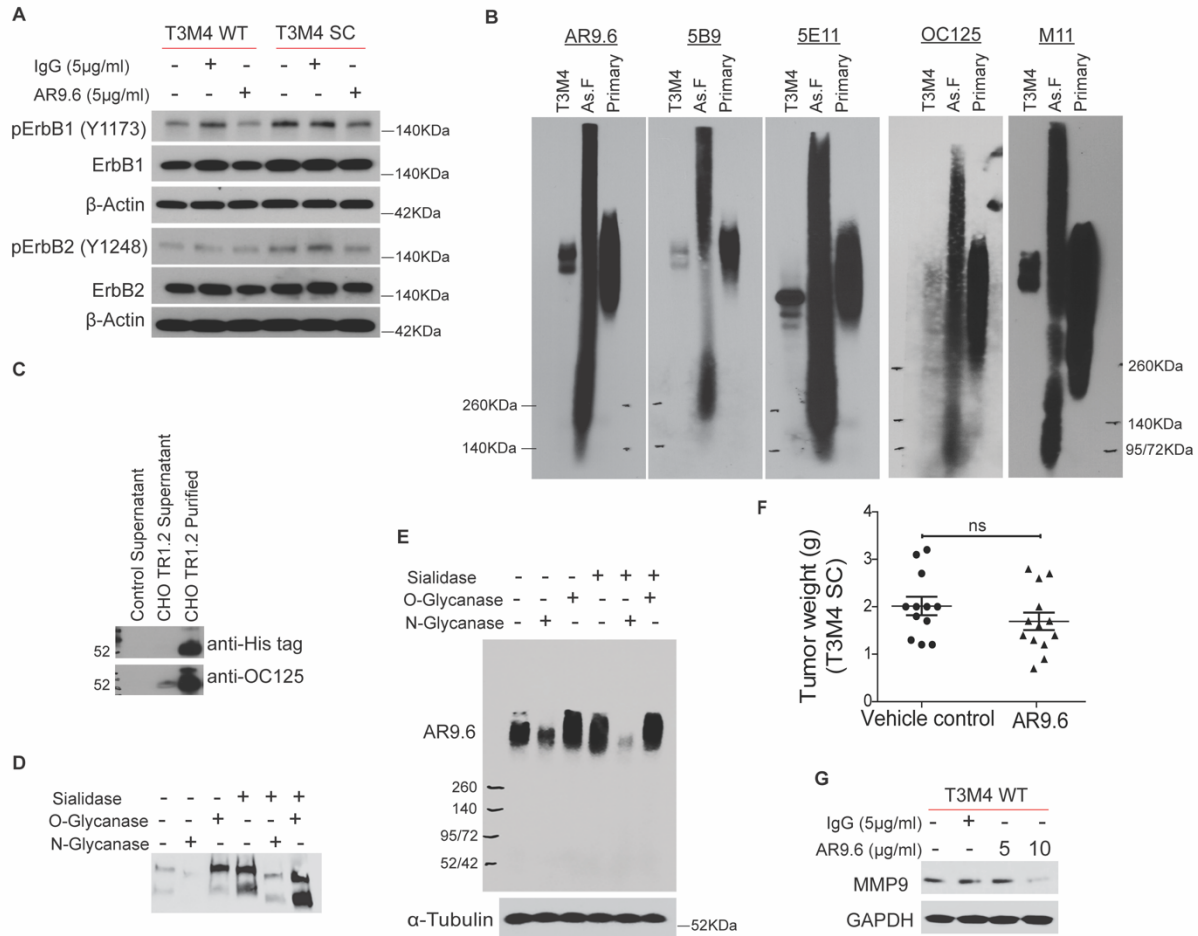
Supplemental Figure S1. MUC16 expression in PDAC. **A.** MUC16 mRNA expression and PDAC patient survival probability was analyzed from the Human Protein Atlas. Kaplan-Meier plot evaluated survival probability of patients expressing low MUC16 (n=54) and high MUC16 (n=122). A significant difference was observed between the two groups at $p=0.0041$ (log-rank test). **B.** Histscore of IHC analysis of MUC16 expression in selected RAP patients with multiple metastatic sites (n=4) using MUC16 specific mAb AR 9.6. **C.** Representative images of IHC analysis of MUC16 expression in selected RAP patients with multiple metastatic sites using MUC16 specific mAb AR 9.6. Scale bar = 40 μ m. **Genetic deletion of MUC16 in PDAC cells. D-F.** CRISPR/Cas9 mediated genetic deletion of MUC16 in T3M4 and Capan-2 (WT and SC) cells and detected by genomic DNA PCR. Parental cells show amplification of a band at 3000bp, which was deleted in MUC16^{KO} clones of PDAC cells. **G.** Western blotting analysis of MMP9 in T3M4 WT, WT-MUC16^{KO}, SC and SC-MUC16^{KO} cells. Detection of β -actin served as the loading control.

Supplementary Figure 2



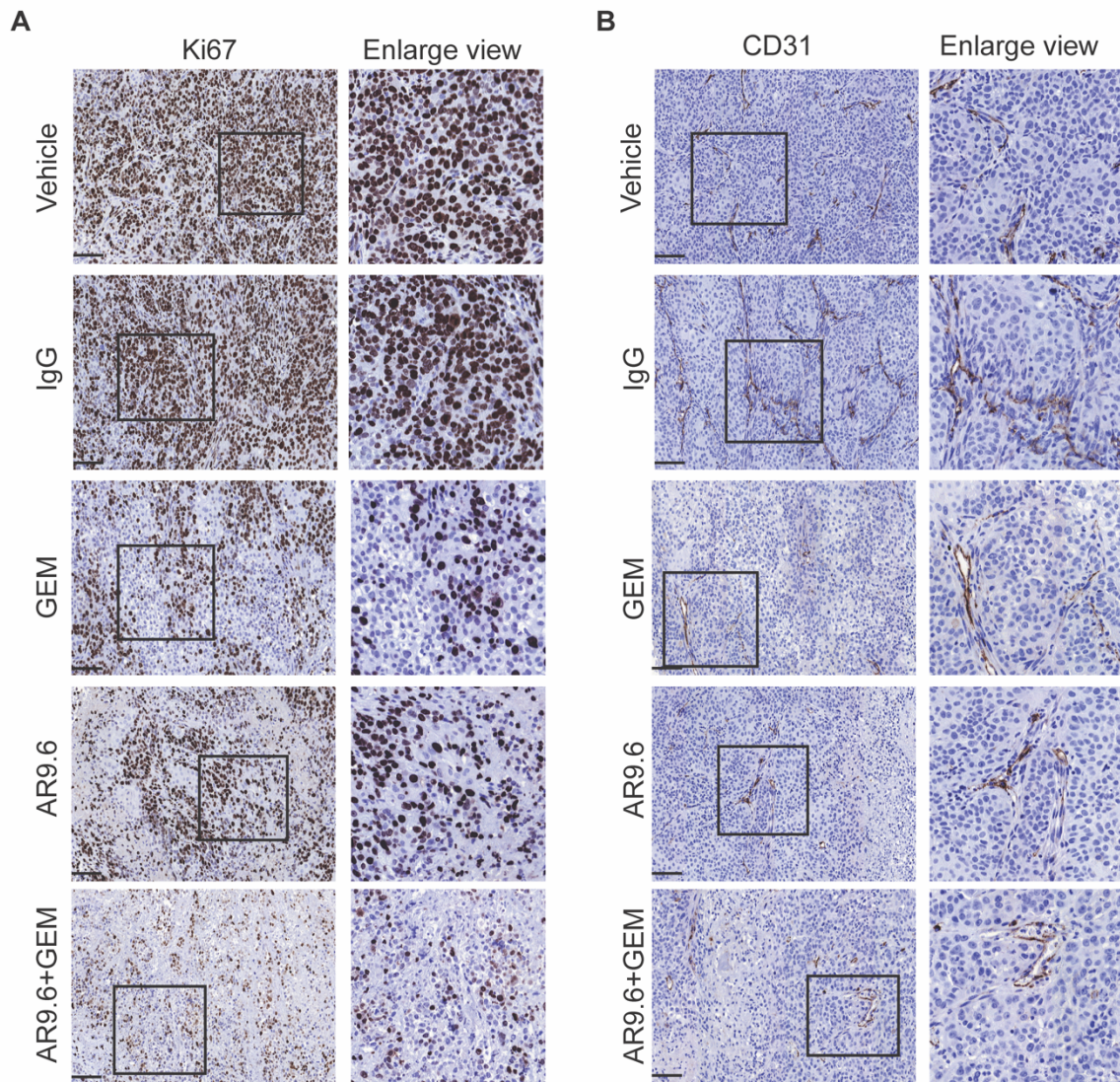
Supplemental Figure S2. Interaction of MUC16 with ErbB receptors. **A.** Western blotting analysis of p-ErbB3 (Y1289), ErbB3, p-ErbB1 (Y1173) and ErbB1 in T3M4 and Capan-2 WT and SC cells. **B.** Western blotting analysis of p-AKT (S473), AKT, p-GSK3β (S9) and GSK3β in T3M4 and Capan2 WT and SC cells. **C.** Western blotting analysis of p-ErbB3 (Y1289), ErbB3, p-ErbB2 (Y1248) and ErbB2, p-AKT (S473), AKT, p-GSK3β (S9) and GSK3β in T3M4WT-MUC16^{KO} cells treated with purified MUC16 (5 μg/ml for 24 h) from PDAC patients (n=5). Detection of β-actin served as the loading control.

Supplementary Figure 3



Supplemental Figure S3. Characterization of MUC16 TR1.2 epitope. **A.** Western blotting of p-ErbB1 (Y1173), ErbB1, p-ErbB2 (Y1248) and ErbB2 in mAb AR9.6 treated T3M4 WT and SC cells. **B.** SDS-agarose western blotting analysis of MUC16 in T3M4 cells lysate, ascetic fluid (As.F) (RAP # 81) and pancreas tumor tissue lysates (RAP # 35) from the PDAC patients samples using MUC16 specific antibodies mAb AR9.6, 5B9, 5E11, OC125 and M11. **C.** MUC16 TR1.2 purified from CHO cells and probed with anti-His-tag and OC125 antibodies. Treatment of MUC16 TR1.2 glycopeptides (**D**) and T3M4 cell lysates (**E**) with Sialidase, O-Glycanase and N-Glycanase, and probed with AR9.6 mAb. Detection of α -tubulin served as the loading control. **F.** T3M4 SC cells implanted tumor-bearing animals were treated with Vehicle control (n=12) and mAb AR9.6 (n=13). [ns, not significant]. **G.** Western blotting analysis of MMP9 in vehicle, mouse IgG and mAb AR9.6 treated T3M4 cells. Detection of β -actin and GAPDH served as the loading control.

Supplementary Figure 4



Supplemental Figure S4. mAb AR9.6 plus Gemcitabine treatment reduces *in vivo* tumor growth. Representative images of immunohistochemical analysis of Ki-67 (A) and CD31 (B) in T3M4 tumor-bearing mice treated with PBS, IgG, gemcitabine, mAb AR9.6, and mAb AR9.6 plus Gemcitabine (n=9).

Supplemental Tables

Table S1. Clinical information of UNMC Rapid Autopsy Pancreas Cancer Patients

RAP #	Age	Sex	Survival days
03	78	F	274
04	59	M	110
05	65	F	35
06	62	M	549
07	71	M	225
08	72	M	9
09	69	M	198
10	74	M	85
11	80	M	185
12	82	M	364
13	72	M	42
16	70	M	178
19	65	M	145
20	77	M	309
21	60	F	221
25	74	M	206
29	80	F	100
30	55	M	148
31	79	M	21
32	59	M	288
33	50	M	228
35	62	M	419
37	58	M	293
39	75	M	65
40	62	M	336
44	58	F	386
46	78	F	71
50	47	F	276
51	57	M	1422
53	57	M	443
54	68	M	168
55	55	F	669
56	74	M	364
57	56	M	51
58	60	M	646
59	62	F	495
61	78	M	269
62	75	M	203

63	70	M	865
64	55	M	423
66	56	M	247
68	66	M	635
72	78	M	366
73	52	M	191
77	80	M	394
78	63	M	451
81	60	F	182
82	71	M	595
85	67	M	446
86	43	M	64
87	56	M	409
88	67	M	227
91	54	M	2011
94	80	M	2282
97	67	M	217
99	70	M	966
100	61	M	1228
101	64	F	725
104	53	M	263
105	89	F	26
109	64	M	405
119	85	F	183
120	69	M	507
123	74	M	90
125	49	F	27
127	81	M	150
129	75	F	427
130	70	M	15
131	72	M	1360
132	77	F	75
133	64	F	1176
135	84	M	893

Table S2. Statistical comparison of IHC histoscores between different anti-MUC16 antibodies.

Trial	N Obs	N	Mean	Std Dev	Median	Minimum	Maximum	P value when Comparing with OC125	Overall P value
OC125	61	61	0.84	1.00	0	0	3.00	Ref	0.002
AR9.6	61	61	1.34	1.18	1	0	3.00	<0.0001	
5B9	61	61	1.15	1.03	1	0	3.00	0.016	
5E11	61	61	0.92	1.00	1	0	3.00	0.40	

UNMC RAP PDAC patients samples. The intensity data were summarized using median value since the data does not follow normal distribution. The Friedman test showed significant differences in the median intensities among at least two of the four antibodies in the studied samples ($p=0.002$). Specifically, the antibody 5E9 (p value=0.016) and AR9.6 (p value<0.0001) shows significantly higher values than OC125.

Table S3. PDAC subtype classification

Classification	Subtype	MUC16
Bailey	Squamous vs Immunogenic	0.00057506
	Squamous vs Progenitor	5.31E-05
	Squamous vs ADEX	8.97E-05
	Immunogenic vs Progenitor	4.24E-01
	Immunogenic vs ADEX	6.66E-01
	Progenitor vs ADEX	7.51E-01
Collisson	Classical vs Exocrine-like	0.8659441
	Classical vs Quasimesenchymal	0.09727453
	Exocrine-like vs Quasimesenchymal	0.05695079
Moffit	Basal-like vs Classical	2.89E-11

Mann-Whitney rank-sum test was used between the PDAC subtype classification system. A p value of less than 0.01 was considered statistically significant.

Table S4. The incidence of tumor metastasis.

T3M4 Cells	Peritoneum	Diaphragm	Lymph node	Liver	Lung	Invaded spleen
WT	35.71% (5/14)	28.57% (4/14)	21.42% (3/14)	42.85% (6/14)	21.42% (3/14)	85.71% (12/14)
WT-MUC16 ^{KO}	21.42% (3/14)	7.1% (1/14)	14.28% (2/14)	7.1% (1/14)	0% (0/14)	42.85% (6/14)
SC	64.28% (9/14)	50% (7/14)	57.14% (8/14)	57.14% (8/14)	42.85% (6/14)	85.71% (12/14)
SC-MUC16 ^{KO}	14.28% (2/14)	7.1% (1/14)	14.28% (2/14)	0% (0/14)	0% (0/14)	28.57% (4/14)
WT vs WT-MUC16^{KO}	<i>0.99</i>	<i>0.98</i>	<i>0.99</i>	<i>0.23</i>	<i>0.66</i>	<i>0.054</i>
WT vs SC	<i>0.39</i>	<i>0.74</i>	<i>0.16</i>	<i>0.99</i>	<i>0.99</i>	<i>0.99</i>
SC vs SC-MUC16^{KO}	<i>0.02</i>	<i>0.099</i>	<i>0.054</i>	<i>0.006</i>	<i>0.048</i>	<i>0.007</i>

Chi-square test or Fisher's exact test was used to compare incidence of tumor metastasis between the following groups: WT vs WT-MUC16^{KO}, WT vs SC, and SC vs SC-MUC16^{KO}. Bonferroni's correction was used for multiple comparisons. A p-value of < 0.05 was considered statistically significant

Table S5. Ingenuity Pathway Analysis (IPA).

Top Canonical Pathways		
Name	p-value	Ratio
Molecular Mechanisms of Cancer	1.4E-16	12/381 (0.031)
B Cell Receptor Signaling	3.04E-16	10/171 (0.058)
ErbB2-ErbB3 Signaling	6.56E-16	8/60 (0.133)
14-3-3-mediated Signaling	2.05E-15	9/121 (0.074)
Prostate Cancer Signaling	1.54E-14	8/99 (0.081)

Previous global profiling of phosphoprotein expression patterns and signal transduction pathways of cells with enforced deletion of COSMC revealed a constitutive activation of steady-state oncogenic signaling cascades¹. Examination of those data by IPA and deductive reasoning identified ErbB2-ErbB3 and FAK as principal nodes for many of the observed effects of truncated O-glycosylation on tumor malignancy.

Supplemental Methods

PDAC Patients Survival Analysis

MUC16 mRNA expression and PDAC patient's survival was analyzed from Human Protein Atlas: <https://www.proteinatlas.org/ENSG00000181143-MUC16/pathology/tissue/pancreatic+cancer> based upon the data generated by the TCGA Research Network. Kaplan plot and the log-rank *p-value* was generated with patients with low MUC16 expression (n=54) and patients with high MUC16 expression (n=122).

LCM-RNA sequencing of Epithelial and Stromal PDAC tissues

Sample acquisition

Freshly frozen tissue samples of PDAC were obtained from surgical specimens from patients undergoing surgery at Pancreas Center at Columbia University Medical Center. Prior to surgery, all patients provided informed consent, which was approved by the local Institutional Review Board (IRB protocol #AAAB2667). Immediately after surgical removal, the specimens were sectioned and microscopically evaluated by the Columbia University Tumor Bank. Suitable samples were transferred into optimal cutting temperature (OCT) medium (Tissue Tek) and snap frozen in a 2-methylbutane dry ice slurry. The tissue blocks were stored at -80°C until further processing. PDAC samples in the Tumor Bank were screened for diagnosis, purity, and viability by H&E analysis of frozen blocks. The overall sample RNA quality was initially assessed by gel electrophoresis; samples exhibiting high RNA quality were utilized for subsequent analyses.

Sample extraction

Frozen tissue specimens were cut at 8 to 9µm thickness and 2 to 3 sections were transferred onto a polyethylene naphthalate membrane glass slide (Arcturus, Applied Biosystems). For initial histopathological review, immediately adjacent sections were cut and stained using a standard Hematoxylin and Eosin protocol to confirm the diagnosis and selected regions of interest.

Laser capture microdissection

Throughout the staining procedure, RNase-free water was used. Fixation was done with 95% ethanol, followed by Crystal violet acetate staining (1% in Tris-buffered 70% ethanol), a brief washing step in 70% ethanol and final dehydration in 100% ethanol. Laser capture microdissection was performed on a PALM MicroBeam microscope (Zeiss) to collect at least 1000 cells per compartment from selected (pre-)malignant areas.

RNA

RNA was extracted using the RNeasy Plus Micro Kit (Qiagen, USA) following the manufacturer's instructions. Prior to processing further, RNA integrity and yield were determined using the Agilent 2100 Bioanalyzer (RNA 6000 Pico Kit for LCM and RNA 6000 Nano Kit for bulk samples, respectively). Yields ranged from 1 to 10 ng per LCM sample and several µg per bulk sample, respectively. Only samples with an RNA Integrity Number (RIN) of at least 7 were used for further processing.

RNA amplification and library preparation

1 - 2 ng of RNA from LCM samples were amplified using the Ovation RNA-Seq System V2 Kit (NuGEN, CA, USA) following the manufacturer's instructions. The resulting cDNA libraries were fragmented using a Covaris S2 Sonicator, and then prepared for the Illumina HiSeq 2000 platform using a Beckmann-Coulter Roboter and the SPRIworks Fragment Library Kit I. Finally, a PCR using the KAPA PCR Amplification Kit was carried out. The libraries were then sequenced at the Columbia Genome Center to generate 30 million single-end reads of 100 bp length.

RNA-Seq analysis

Gene and isoform abundances were estimated using RSEM (with read alignment being performed by the STAR aligner) and RefSeq gene annotations (GRCh38). Differential gene expression analysis was carried out at the gene level using the edgeR and limma R packages and the Voom framework implemented therein ².

Sample Numbers

A total of 242 epithelial samples out of which 197 from primary PDAC, 26 from low-grade PanIN, and 19 from low-grade-IPMN; and a total of 159 stromal samples (matched with epithelium) out of which 124 from primary PDAC, 23 from low-grade PanIN, and 12 from low-grade IPMN were used for the study.

MUC16 expression in different subtypes of PDAC

Consensus clustering was applied on all 150 TCGA PAAD tumor samples ³ using the gene sets from Collisson et al ⁴, Moffitt et al ⁵ and Bailey et al ⁶, classifying the samples into three subtypes (classical (n=54), quasimesenchymal (n=34), or exocrine-like (n=62)), two subtypes (basal-like (n=65) or classical (n=85)) and four subtypes respectively (squamous (n=31), immunogenic (n=28), pancreatic progenitor (n=53), or aberrantly differentiated exocrine [ADEX] n=38)). Then, the Mann-Whitney rank-sum test was used for comparing MUC16 expression among subtypes.

Genomic DNA Amplification

Total DNA was extracted from T3M4 WT, WT-MUC16^{KO}, T3M4 SC, SC-MUC16^{KO} cells using Promega Wizard® genomic DNA purification kit according to the manufacturer's instructions. 100ng of total genomic DNA was amplified by PCR using Phusion™ High-Fidelity DNA Polymerase (ThermoFisher Scientific, USA) according to the manufacturer's instructions with the following primers: MUC16 FP 5'-TGGTCATTTCTGAGTGTGGAA-3', MUC16 RP 5'-CTCCACATCACCAGAGAGCA-3' (Integrated DNA Technologies, USA). PCR conditions were 39 cycles at 95°C for 5 min, 95°C for 30 sec, 60.5°C for 30 sec, 72°C for 5 min. the amplified samples were detected by 1% agarose gel electrophoresis.

SDS-Agarose electrophoresis

SDS-Agarose gel electrophoresis for MUC16 was performed as described previously ⁷ with minor modifications. Briefly, T3M4 WT, WT-MUC16^{KO}, T3M4 SC, SC- MUC16^{KO} cell lysates [RIPA lysis buffer (Thermo Scientific, Rockford, IL USA) with protease and proteinase inhibitor] were resolved on SDS (0.1%) - Agarose (2%) gel electrophoresis (50-100 µg/lane) and transferred to PVDF membrane by capillary transfer. After blocking the membranes in 5% skimmed milk in TBS-T (Tris-buffered saline and 0.1% Tween 20, pH 7.4), the membranes were probed with mouse anti-MUC16 abs, AR9.6 (Quest PharmaTech, Canada), 5B9 and 5E11 (Provided by Dr. Ulla Mandel, University of Copenhagen, Denmark), OC125 (Covance, USA), M11 (LSBio, USA) and mouse anti- α -tubulin IgG (Developmental studies hybridoma bank, Iowa, USA) overnight. The membranes were washed with TBS-T and incubated with HRP conjugated Goat-anti mouse secondary antibody (Jackson ImmunoResearch, West Grove, PA, USA). The antigen-antibody complex was detected with enhanced Chemiluminescent kit (Bio-rad, USA).

Deglycosylation of TR1.2 and MUC16

MUC16 TR1.2 glycopeptides were expressed and purified as described earlier ⁸. Deglycosylation of purified MUC16 TR1.2 glycopeptides and MUC16 positive T3M4 cell lysate was performed by using deglycosylase cocktails containing Sialidase, O-glycanase, and N-glycanase (Prozyme, Hayward, CA, USA) as per the manufacturer instructions. Deglycosylated TR1.2 glycopeptides and T3M4 cell lysates were immunoprobed with mAb AR9.6, as described above.

Isolation and purification of MUC16 from Patient's ascites fluid

MUC16 was isolated and purified from Patient's ascites fluid using standard affinity column chromatography method as described previously with modifications ⁹. Briefly, ascites fluid (10ml) was centrifuged at 1000g for 30 seconds

and mixed with protein L-resin (GenScript, USA) for 2 hours at room temperature and collected the supernatant by centrifuging at 1000g for 30 seconds. The supernatant was then passed through monoclonal antibody mAR9.6 (1mg/200 μ l) along with protein G resin (GenScript, USA) conjugated affinity chromatography column (Thermo Scientific, Rockford, IL USA). After washing out non-bound debris with PBS, the antigen was eluted from the antigen-antibody complex with acidic elution buffer (0.1M glycine-HCl, pH 2.8); neutralized with neutralization buffer (1M Tris-HCl pH 8.5); and dialyzed against PBS. The purified MUC16 antigen was used for the treatment studies.

Expression and purification of MUC16 TR1.2 in CHO cells

MUC16 TR1.2 was expressed and purified from CHO cells as described previously⁸. Briefly, CHO cells were grown in medium containing 80% EX CELL CHO Cloning Medium (Sigma) and 20% EX CELL CD CHO Fusion medium (Sigma) with 2% glutamine and 0.32 mg/mL G418 (Invitrogen). The cells were stably transfected with 3 μ g of pcDNA3- γ -MUC16 TR1.2 construct encoding for a fragment with 124 aa with a C-terminal myc tag and N- and C-terminal 6xHis tags using LipofectamineTM Transfection Reagent (ThermoFisher, USA). Positive clones were selected by screening the expression of His-tag protein with anti-His (Invitrogen, USA) or anti-MUC16 OC125 (). The secreted MUC16 TR1.2 (His-tag) was purified by cobalt column chromatography (TALONTM) as per the manufacturer's instruction.

References:

1. Radhakrishnan, P., Dabelsteen, S., Madsen, F.B., Francavilla, C., Kopp, K.L., Steentoft, C., Vakhrushev, S. Y., Olsen, J. V., Hansen, L., Bennett, E.P., et al. (2014). Immature truncated O-glycophenotype of cancer directly induces oncogenic features. *Proc Natl Acad Sci U S A.* 111, E4066-E4075.
2. Law, C.W., Chen, Y., Shi, W., Smyth, G.K. (2014). voom: Precision weights unlock linear model analysis tools for RNA-seq read counts. *Genome Biol.* 15, R29.
3. Cancer Genome Atlas Research Network. Electronic address: andrew_aguirre@dfci.harvard.edu; Cancer Genome Atlas Research Network (2017). Integrated Genomic Characterization of Pancreatic Ductal Adenocarcinoma. *Cancer Cell.* 32, 185-203.e13.
4. Collisson, E.A., Sadanandam, A., Olson, P., Gibb, W.J., Truitt, M., Gu, S., Cooc, J., Weinkle, J., Kim, G.E., akkula, L. et al. (2011). Subtypes of pancreatic ductal adenocarcinoma and their differing responses to therapy. *Nat Med.* 17, 500-503.
5. Moffitt, R.A., Marayati, R., Flate, E.L., Volmar, K.E., Loeza, G.H., Hoadley, K.A., Rashid, N.U., Williams, L.A., Eaton, S.C., Chung, A.H. et al. (2015). Virtual microdissection identifies distinct tumor- and stroma-specific subtypes of pancreatic ductal adenocarcinoma. *Nat Genet.* 47, 1168-1178.
6. Bailey, P., Chang, D.K., Nones, K., Johns, A.L., Patch, A.M., Gingras, M.C., Miller, D.K., Christ, A.N., Bruxner, T.J.C., Quinn, M.C. et al. (2016). Genomic analyses identify molecular subtypes of pancreatic cancer. *Nature.* 531, 47-52.
7. Gabriel, M., and Zentner, A. (2005). Sodium dodecyl sulfate agarose gel electrophoresis and electroelution of high molecular weight human salivary mucin. *Clin Oral Investig.* 9, 284-286.
8. Marcos-Silva, L., Narimatsu, Y., Halim, A., Campos, D., Yang, Z., Tarp, M.A., Pereira, P.J., Mandel, U., Bennett, E.P., Vakhrushev, S.Y., et al. (2014). Characterization of binding epitopes of CA125 monoclonal antibodies. *J Proteome Res.* 13, 3349-3359.
9. Lloyd, K.O., Yin, B.W., Kudryashov, V. (1997). Isolation and characterization of ovarian cancer antigen CA 125 using a new monoclonal antibody (VK-8): identification as a mucin-type molecule. *Int J Cancer.* 71, 842-850.